Passive margin evolution and controls on natural gas leakage in the Orange Basin, South Africa

Article *in* South African Journal of Geology · December 2011

DOI: 10.2113/gssajg.114.3-4.415

PASSIVE MARGIN EVOLUTION AND CONTROLS ON NATURAL GAS LEAKAGE IN THE ORANGE BASIN, SOUTH AFRICA

D. BOYD
AEON (Africa Earth Observatory Network) and University of Cape Town, Rondebosch, 7701, South Africa
e-mail: boyd.donna@gmail.com

Z. ANKA
GFZ German Research Centre for Geosciences, Telegrafenberg, 14473, Potsdam, Germany
e-mail: zahie@gfz-potsdam.de

R. DI PRIMIO
GFZ German Research Centre for Geosciences, Telegrafenberg, 14473, Potsdam, Germany
e-mail: dipri@gfz-potsdam.de

G. KUHLMANN
BGR, Bundesanstalt für Geowissenschaften und Rohstoffe (BGR), Wilhelmstr. 25-30, D-13593 Berlin, Germany
e-mail: Gesa.Kuhlmann@bgr.de

M.J. DE WIT
AEON and Centre for Earth Stewardship Science, Nelson Mandela Metropolitan University, Port Elizabeth, South Africa,
e-mail: maarten.dewit@nmmu.ac.za

ABSTRACT

Throughout exploration Block 2 of the Orange Basin offshore the South African continental margin, different natural gas leakage features and the relationship between natural gas leakage with structural and stratigraphic elements were studied. This study also quantifies liquid/gas hydrocarbon generation, migration and seepage dynamics through the post-rift history of the basin.

The interpretation of seismic data reveals two mega-sequences: Cretaceous and Cenozoic that are subdivided by major stratigraphic unconformities into 5 and 2 sub-units, respectively. The basin is also divided into 2 structural domains:

1. an extensional domain characterized by basinward dipping listric normal faults rooted at the Cenomanian/Turonian level identified between 500 to 1500 m of present-day depth,
2. a compressional domain that accommodates the up-dip extension on the lower slope, and which is characterized by landward dipping thrust faults.

One hundred and thirteen observed gas chimneys are identified and classified into stratigraphically-controlled (sa-c) and structurally-controlled (s-c) chimneys. The ratio of s-c versus s-ac chimneys is estimated as 2:5, which suggest a strong stratigraphic control on natural gas leakage. The chimneys either terminate at the seafloor where active leaking gas is manifested by pockmarks, or are sealed within the Miocene (14 Ma) sequence as paleo-pockmarks. The s-c chimneys are located along the normal faults in the extensional domain, and terminate as seafloor mounds up to 1500 m in diameter and with heights between 10 to 50 m. The sa-c pockmarks range between 100 to 400 m in diameter, and are linked to stratigraphic onlaps and pinch-outs within the Aptian sequence. Several giant chimneys, with diameters of more than 7 km, are also identified. At least one of these displays apparent internal gravitational collapse structures. Bright spots indicative of gas presence within these large chimneys were identified, but there is no evidence of acoustic turbidity or seismic pull-downs within these large structures. This suggests the giant chimneys are inactive paleo-gas-escape structures.

Modelling suggests that gas from the lower Aptian and the Barremian source rocks migrates laterally-updip to the proximal parts of the basin where it accumulates beneath the Cenomanian/Turonian sequence that acts as a regional seal. Across the shelf-break and the upper slope, chimneys and pockmarks are fed from younger Cenomanian/Turonian source rocks. The migration model also indicates that fluids are about 24 times more likely to flow out of the study area than to be preserved within it.

Since methane gas escaping across the sea floor into the exosphere (combined hydrosphere and atmosphere) may contribute to Earth's climate fluctuations, and because escaping gas must have been cut off when at least half of identified s-c chimneys were sealed within the Miocene sequence, decrease of gas escape along the southern African continental margin may have to be factored into global Neogene cooling models.

SOUTH AFRICAN JOURNAL OF GEOLOGY, 2011, VOLUME 114.3-4 PAGE 349-366
doi:10.2113/gssajg.114.3-4.349

Introduction

Sedimentary basins offshore passive continental margins are potential hydrocarbon storehouses where liquid and gaseous hydrocarbons accumulate in reservoirs buried across these margins. One of the most common gaseous hydrocarbon found in sedimentary basins is CH_4 - methane (Whiticar 1989; Judd et al., 2002; Kennett et al., 2002; Milkov 2004). In many cases, such as well described along the continental shelf of Norway (Brendt, 2005; Svensen et al., 2003; Bunz et al., 2005; Mazinni et al., 2006), in the Black Sea (Dimitrov, 2002) and the Sea of Okhotsk (Cranston et al., 1994), methane escapes across the sea floor via carbonated gas seeps and mud volcanoes, into the exosphere (e.g. the hydrosphere and atmosphere) where it eventually oxidizes to form CO_2 (e.g. Kennett et al., 2002; Etiope and Klusman 2002 and Judd et al., 2002). Because methane is at least twenty times more potent than CO_2 as a greenhouse gas, its storage and/or escape may greatly affect exosphere temperatures (Kennett et al., 2002; Etiope et al., 2008; Wuebbles et al., 2002; Svensen et al., 2004; Zachos et al., 2008).

Recent work based on past episodes of global warming provide insights into the coupling of climate and the carbon cycle (van de Schootbrugge et al., 2008; McElwain et al., 2009), which in turn may help to differentiate natural from anthropogenic contributions to carbon emissions. For example, sudden palaeo-release of geologically stored methane is believed to have been responsible for episodic rapid rises in global temperatures and changes in climate (i.e. Whiticar 1989; Kennett et al., 2002; Dickens 2003; Svensen et al., 2004; Zachos et al., 2008). It has been suggested that a rapid or catastrophic release of methane might have happened around 55 Ma, catalyzing the Paleocene-Eocene Thermal Maximum (PETM), when global temperature increased by ~5°C in perhaps less than 10,000 years (Kennett et al., 2002; Svensen et al., 2004; Zachos et al, 2008). The tell-tale signs of such event are increased acidification of the ocean and sudden carbon isotopic excursions likely due to the injection of a very large mass of ^{13}C- depleted carbon into the atmosphere (Dickens 1995 and 2003; Kennett et al., 2002; de Wit et al., 2002; Svensen et al., 2004; van de Schootbrugge et al., 2008; Zachos

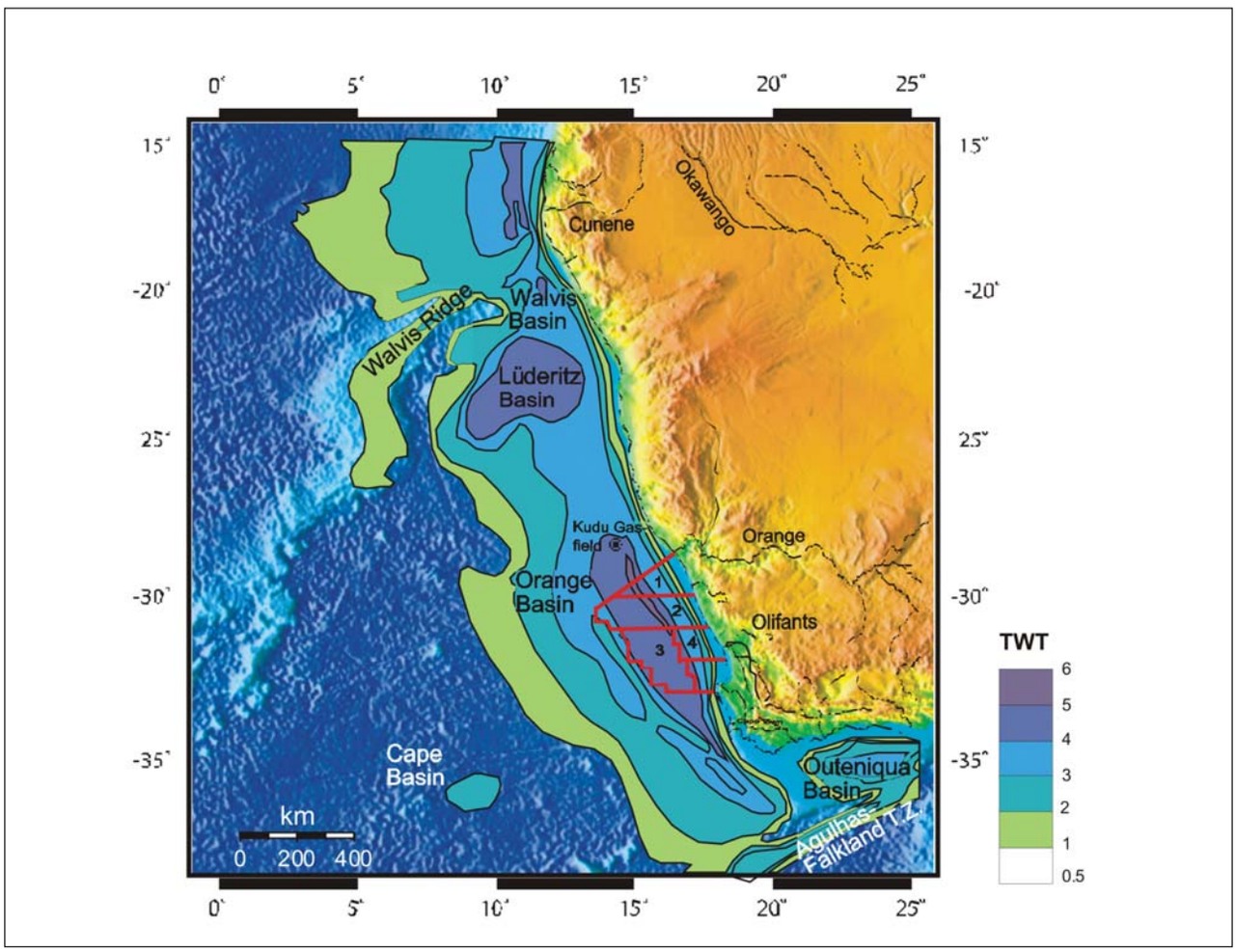

Figure 1. *A physiographic map with the superimposed isopach maps (TWT of sediment thickness) showing the Orange Basin. The basin offshore of southern Africa between the Walvis ridge in the north and the Agulhas-Falkland Transform Zone in the south [modified from Kuhlmann et al., (2010)]. Exploration blocks 1 to 4 (red lines) are shown. The study area covers exploration Block 2 of the Orange Basin.*

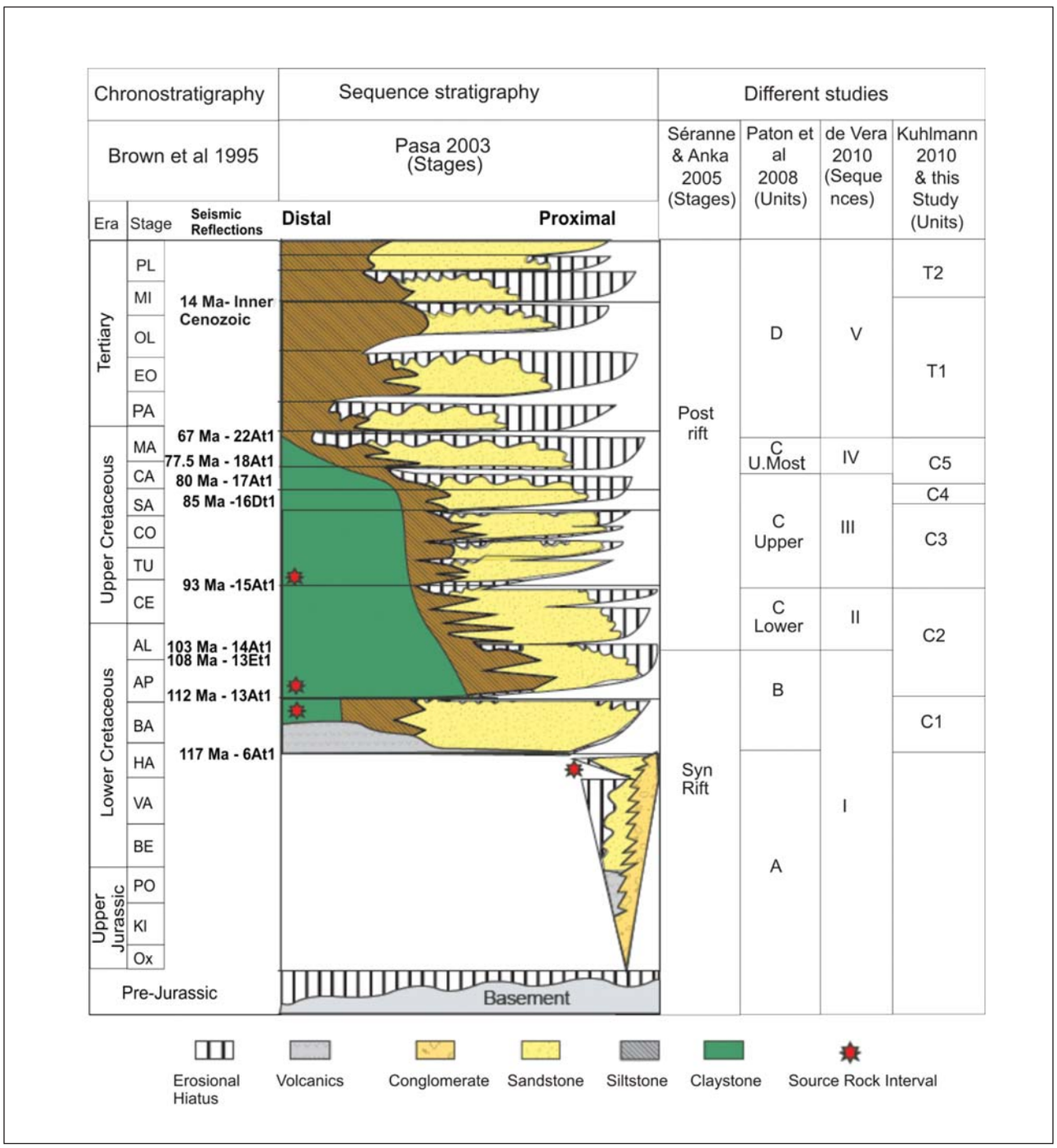

Figure 2. *Chronostratigraphic and sequence chart for the Orange Basin showing the major seismo-stratigraphic units and their bounding unconformities according to different authors (Brown et al., 1995; Séranne and Anka., 2005; Paton et al., 2008; de Vera at al., 2010; Kuhlmann et al., 2010)*

et al., 2008; McElwain et al., 2009). Whilst the source of the carbon may derive from dissociation of near surface clathrates (methane hydrates) along continental margins (e.g. Kennett et al., 2002; Dickens 1995 and 2003), it is not known with any degree of certainty if methane release from deeper gas reservoirs within sedimentary basins also contributes to such events (e.g. Svensen et al., 2004; Brendt 2005). Amongst the mechanisms resulting in clathrates dissociation, increase in sea water temperatures, in concert with associated positive feedbacks are paramount (Dickens 2003). The consequences lead to an increase in mean global temperature, as recorded in the stratigraphic records (Royer 2006 and Royer et al., 2007).

However, along the continental margin of southern Africa, the onset of the cold Benguela current following the opening of the Drake Passage and emergence of the circumpolar current (e.g. Wiegelt

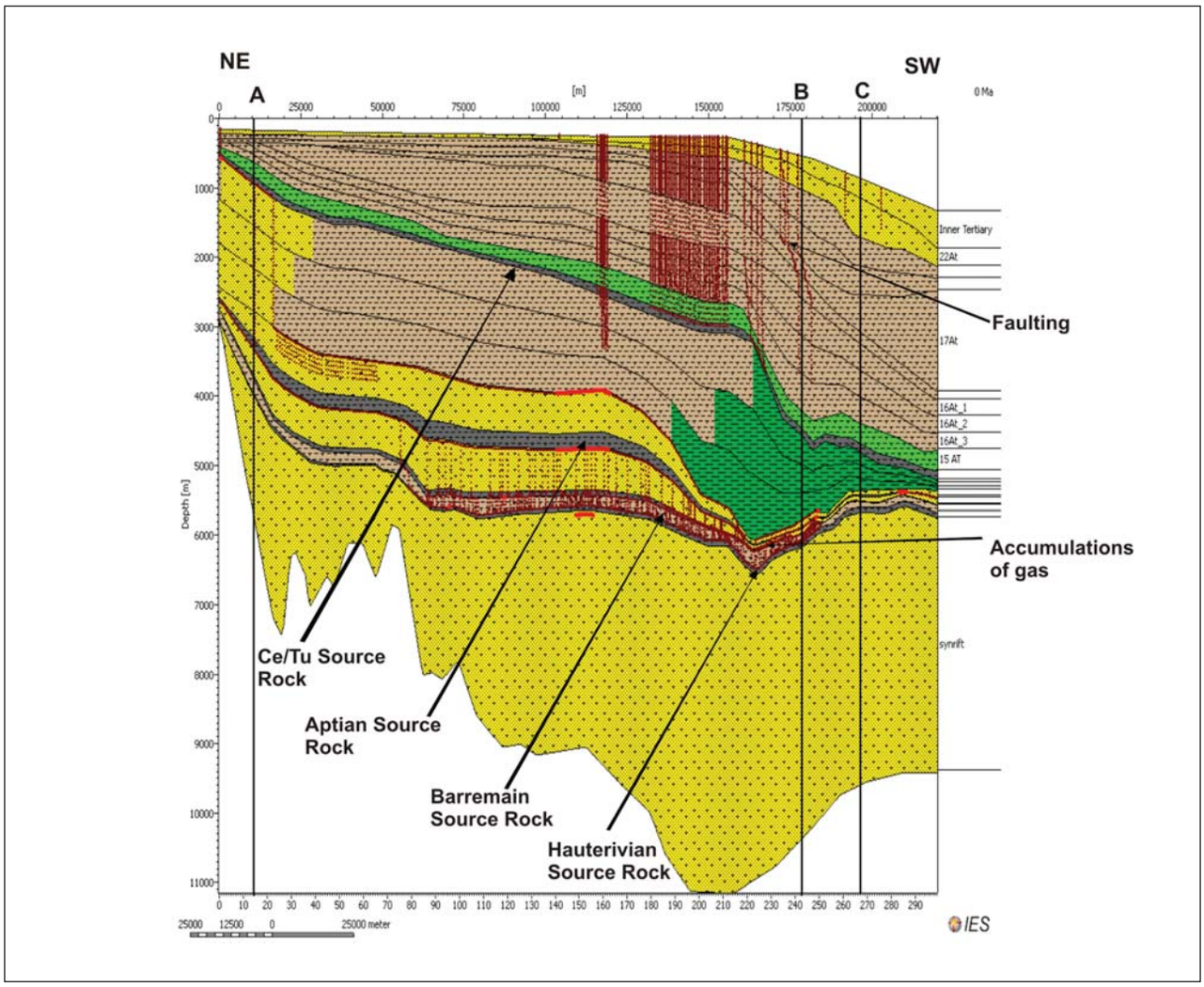

Figure 3. *Depth converted model produced by the composite seismic line (see Figure 4) with facies definition (e.g. Kuhlmann et al., 2010) for each unit. Source rocks are shown in grey (see legend). In addition, a SE trending fault (zigzag lines) is displayed and the three depth extractions from wells (black vertical lines) are shown at the proximal (**A**), middle (**B**) and distal locations (**C**) of the basin at 9,320 m, 182,230 m, and 198,662 m distances, respectively. This model also shows gas migration at the present day. Modelled hydrocarbon migration is shown as maroon dotted lines and can reproduce the associations observed in the seismic data showing identified gas chimneys.*

and Uenzelmann-Neben, 2004; Uenzelmann-Neben et al., 2007) suggests that increasing sea water bottom temperatures cannot have been the catalyst for onset of gas escape features along this margin. Thus a deeper gas-reservoir leakage is more likely to have initiated the gas hydrate and mud volcanoes already identified along the margin (e.g. Ben-Avraham et al., 2002; Viola et al., 2005). Thus, quantification of thermally-driven methane emission from deep hydrocarbon reservoirs along continental margins may provide additional key insights into their potential role in global carbon cycle and climate history. This study is an attempt to address this, by identifying, characterizing and modelling leakage of liquid/gas hydrocarbons in a known gas bearing basin as the Orange Basin, offshore the western South African margin. Our results may help to understand the relationship between methane migration and seepage with structural and stratigraphic elements in this basin, and may also contribute to a better quantification of the fluxes of greenhouse gases from sedimentary basins along this and other continental margins.

Geological setting of the Orange Basin

The Orange Basin, with an area of approximately 130 000 km^2, is located off the south-west facing continental margin of South Africa (Gerrard and Smith., 1982; Dingle et al., 1983; Muntingh 1993; Brown et al., 1995; Paton et al., 2007; Kuhlmann et al., 2010: Figure 1). The basin is bounded to the north and south by the Walvis Ridge and by the Agulhas-Falkland Fracture Zone (Figure 1) respectively and has been filled by sediments transported by the Olifants and Orange River drainage systems since the Mesozoic (Gerrard and Smith., 1982; Dingle et al., 1983; Muntingh 1993; Brown et al., 1995). Due to its economic importance, the Orange Basin is divided into several exploration blocks (Figure 1).

Previous studies were conducted by Paton et al. (2007; 2008) and Kuhlmann et al. (2010) on Blocks 3 and 4, in the southern part of the basin. Our study area comprises Exploration Block 2, which is located in the northern part of the basin and covers an area of approximately 18750 km^2 (Figure 1).

The basin records the development of South Africa's volcanic-rifted passive continental margin from the Late Jurassic to the present (Gerrard and Smith, 1982; Muntingh 1993; Brown et al., 1995: Figure 2). It contains a total thickness of about 7 km of post-rift sedimentary sequences in the northern area and about 3 km-thick sedimentary sequences to the south (Gerrard and Smith, 1982; Brown et al., 1995; Tinker et al., 2008).

It is generally accepted that the present day margin formed during the break-up of Gondwana and the opening of the South Atlantic Ocean during the Late Jurassic to Early Cretaceous (Gerrard and Smith., 1982; Brown et al., 1995; Nurnberg and Muller, 1991; MacDonald et al., 2003; Moulin et al., 2010). More recently, Moulin et al. (2010) had proposed that the first oceanic crust between southern Africa and America formed between magnetic anomalies M9 and M7 (Lower Cretaceous 132 to 134 Ma).

The break-up of Gondwana resulted in the development of a series of grabens and half-grabens oriented parallel to the present-day margin (Gerrard and Smith., 1982; Dingle et al., 1983; Muntingh 1993; Brown et al., 1995; Paton et al., 2007; Kuhlmann et al., 2010). This complex of grabens and half-grabens is separated by a medial hinge from a more distal western wedge of seaward dipping reflectors (Jungslager 1999; Broad et al., 2006). The immediately overlying sedimentary successions consist of deposits of Upper Jurassic and Lower Cretaceous siliciclastic, lacustrine sediment infills with volcanic intrusions (Paton et al., 2007 and Kuhlmann et al., 2010). These deposits are followed by transitional Lower Cretaceous siliciclastic deposits that show a deepening-upward sequence from fluvial red beds to deltaic deposits (Gerrard and Smith, 1982). Full marine conditions set in during the Barremian-Aptian (117 to 103 Ma) in response to the initiation of the main drift phase of the South Atlantic opening that appeared to be regionally developed within the basin (Gerrard and Smith., 1982; Dingle et al., 1983; Muntingh 1993; Brown et al., 1995; Paton et al., 2007; Kuhlmann et al., 2010).

The oldest proven and highest quality source rock interval comprises the syn-rift Upper Hauterivian (around 117 Ma: Figure 2) lacustrine deposits, found within the grabens and half grabens (Jungslager 1999). This source rock is oil-prone, with a TOC (Total Organic Carbon) of more than 10% and HI (Hydrogen Index) of more than 600 mg HC/g TOC (Barton et al., 1993; Muntingh, 1993). Another high quality interval found in the basin is of Barremian to Aptian age (around 112 Ma : Figure 2 : Jungslager 1999 and van der Spuy 2003). This sequence which is up to 300 m thick and TOC values up to 25%, was penetrated by DSDP 361 and corresponds to a major lithofacies change, from restricted marine to open marine conditions (Herbin et al., 1987).

Another source rock interval has been identified within the post-rift Upper Cretaceous succession (Muntingh 1993; Van der Spuy et al., 2003) (Figure 2). This corresponds to an uppermost Cenomanian-Turonian maximum flooding event (93 Ma) that was identified in some wells and is predicted to be oil prone down-dip to the west (Van der Spuy et al., 2003).

Database and methodology

This study analysed a large 2D time-migrated 250 km seismic-reflection dataset that extends for from the margin and the shallow marine domain at 200 m water depth, to the deep marine domain at 3000 m water depth, from the shelf to the abyssal plain of exploration Block 2. More than 300 2D seismic-reflection profiles, both parallel ("strike") and perpendicular ("dip") to the continental margin, and data (well logs and checkshots) from 10 boreholes located on the exploration Block 2 were provided by PASA (Petroleum Agency of South Africa). The length of the seismic profiles ranges from about 12 km to around 125 km. The spacing between the seismic lines varies from 0.8 km to 16 km. Based on seismic interpretation and seismic stratigraphy observations, the main seismic sequences, tectonic structures, and gas/ fluid escape features have been identified, mapped, and classified. These observations form the basis for a further 2D numerical simulation of hydrocarbon generation and migration events. A 3D modelling approach is required but it is beyond the scope of this work.

The seismic reflection analysis was carried using Petrel® Interpretation software (Version 2009.1) of Schlumberger. The seismic reflections were identified, tied to stratigraphic well tops, and mapped. The procedures used before interpretations were general findings and observations of the chimneys and the description of the chimneys are found in the appendix. The true amplitudes were preserved. Two-way travel time (TWT) maps of the horizons and seismic sequence isopach maps were also generated. A large variety of gas leakage indicators such as seafloor pockmarks, seismic chimneys, pipes and mud volcanoes were identified within the seismic data and were then grouped according to their association to structural or stratigraphic elements and their general distribution across the basin. The interpreted TWT horizons were converted to depth, using the available checkshots information from the wells, to create structural and isopach maps in meters, in order to provide the depth information required for 2-D petroleum system modelling. This modelling was carried out, using the commercial software Petromod ® (Version 10) from Schlumberger. It aims to simulate the burial and thermal evolution of the basin, including its hydrocarbon generation and migration processes through time. To accomplish this, a representative 220 km-long and

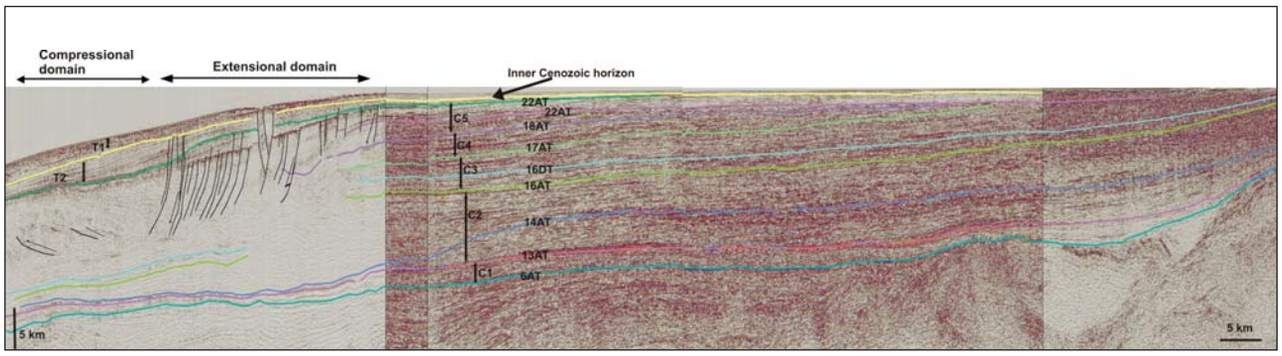

Figure 4. *Composite seismic line showing the main identified seismic units (C1-C5; T1-T2) and their bounding surfaces (seismic horizons). The main structural elements of the basin are: (**i**) an extensional domain, identified in the present-day continental shelf break/upper slope, characterised by shallow-dipping normal listric faults and (**ii**) a compression domain on the continental lower slope, dominated by landward dipping listric thrust faults. Location of this composite-line is shown in Figure 5a.*

~11 km deep northeast to southwest regional transect across the basin was selected (Figure 3).

The main stratigraphic horizons were input into Petromod software by digitizing a bitmap of the depth converted transect, and were then gridded using a constant grid spacing of 735 m resulting in 300 grid points for this model (Figure 3). The number of grid points was adequate to reproduce the main structural features observed in the seismic data. Based on the stratigraphic resolution available, about twenty series of deposition events were defined and further refined by simulating episodes of erosion. The depositional events were also assigned to sedimentary facies that include lithology and, when approximate source rock properties. Lithologic properties were assigned to the individual sequences based on the identified chronostratigraphic and sequences (Figure 2). TOC and HI values of the source rocks (Bray et al., 1998; Muntingh 1993; Jungslager 1999; Ben-Avraham et al., 2002; Van der Spuy 2003; Paton et al., 2007 and 2008; Kuhlmann et al., 2010) as well as the reaction parameters were included.

Kinetic parameters are used to describe the rate of reaction for conversion of kerogen to oil and gas assuming primary and secondary cracking reactions. Reaction parameters in this study were adopted from Pepper and Corvi (1995a; 1995b) and Pepper and Dodd (1995) and assigned to the four source rock intervals of Hauterivian (Kerogen Type I), Transitional Barremian (Kerogen Type III), lower Aptian (Kerogen Type II), and Cenomanian/Turonian (Kerogen Type II).

The following boundary conditions were set to prepare the model for simulations and they define the basic energetic conditions for reconstruction of the temperature and burial history of the study area:

1. PWD (Paleo Water Depth) is determined from a combination of tectonic subsidence and changes in global sea levels to fit the geologic data (e.g. facies concept; Poelchau et al. 1997). Due to the lack of detailed paleo-bathymetric data we assumed a linear evolution through time, starting at from 0 water depth at rift initiation to the present day water depth in our model. The linear interpolation is the most parsimonious assumption in the absence of better data
2. SWIT (Surface Water Interface Temperature) to set the upper temperature boundary through time. Here we used the approach of Wygrala (1989) where SWIT is based on reconstructed sea floor temperatures linked to the latitude of the study area.
3. HF (Heat Flow) evolution through geologic time. The heat flow is based on Paton et al., (2007) and modelled following a McKenzie (1978) type lithospheric stretching model. Our heat flow model assumes a finite instantaneous stretching event at 125 Ma followed by exponential thermal decay over 75 Ma to a steady state, terminating of 60 mW/m^2. Heat flow variability along the modelled section was not deemed significant. Heat flow modelling was calibrated against vitrinite reflectance and temperature data from two wells from Block 3 (Figure 1). These data are based on the kinetics for vitrinite maturation of Sweeney and Burnham (1990). Model calibration was achieved using the above determined heat flow history in conjunction with increasing the temporal and stratigraphic resolution of the model and was further improved by additional modifications, i.e. through adding several more stratigraphic subdivisions and improving the facies variability according to the chronostratigraphic chart.

Once a thermally calibrated model was obtained, final fluid flow and gas migration models were constructed. The results were then compared to and calibrated with the leakage features observed on the seismic section.

Seismic interpretation

Seismo-stratigraphic units

Analysis of the seismic reflection profiles data reveals the existence of seven major seismo-stratigraphic units display the major changes within the basin geometry:

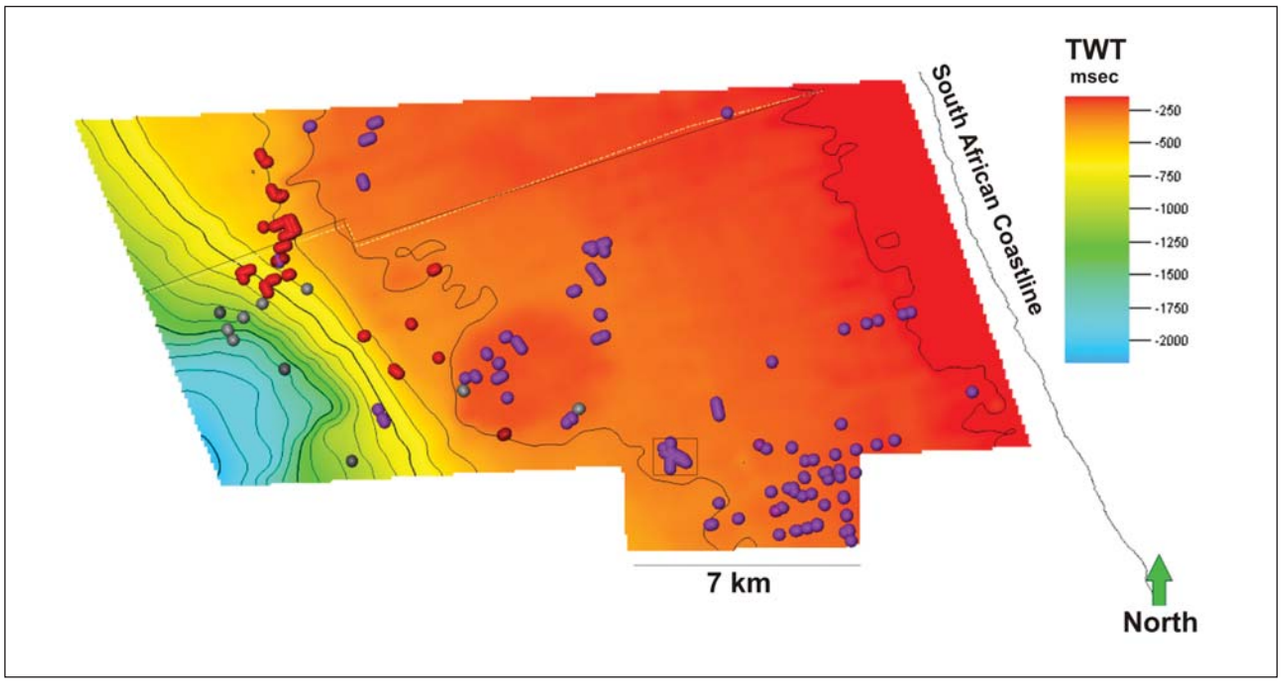

Figure 5. *(**a**) The study area, showing the distribution of three classes of major gas chimneys identified in this study: (purple) stratigraphic controlled chimneys (red) structural controlled chimneys and (grey) paleo chimneys. Note that the structurally-controlled chimneys are confined to the deep basin and steepest slopes, while the stratigraphically-controlled chimneys dominate the middle and upper shelf. The location of a giant collapsed chimney is marked by a black square. The composite regional seismic section depicted in Figure 4 is shown as a bold black line. The green arrow points to the North.*

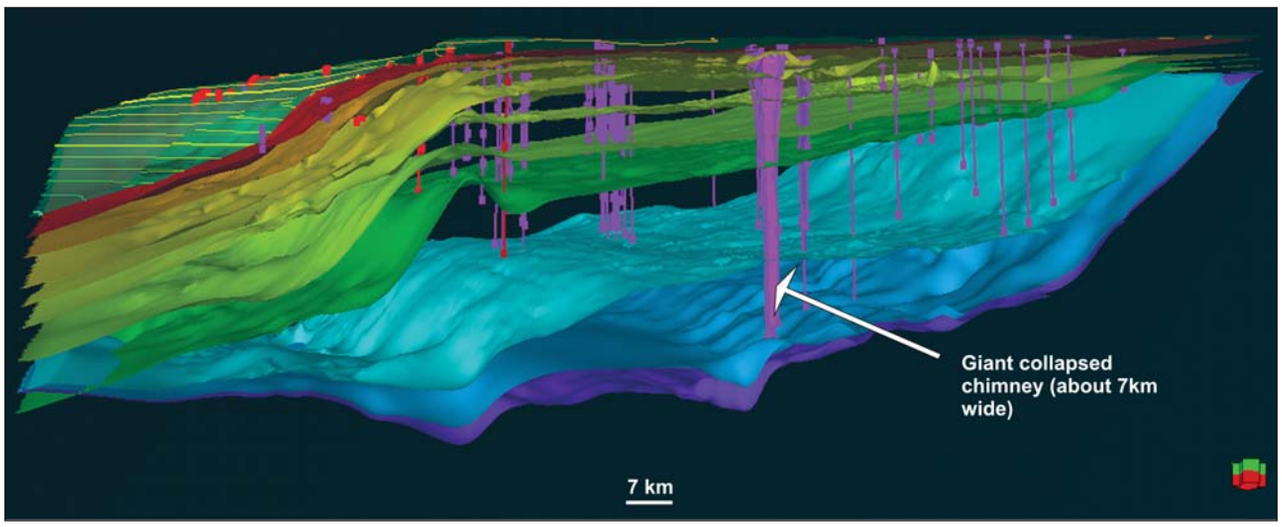

Figure 5. *(**b**) 3D view showing the progradation of the continental margin since Albian (14At). Note that the structurally-controlled chimneys (red) are confined to the extensional domain of the slope, whilst the stratigraphically-controlled chimneys (purple) are confined to the middle and upper shelf (from Petrel software). The bathometry was obtained from the seismic profiles. The arrow points to the North.*

C1 (Barremian- Aptian), C2 (Early Aptian- Cenomanian), C3 (Turonian- Coniacian), C4 (Santonian), C5 (Campanian- Maastrichtain), T1 (Lower Cenozoic from 67 to 14 Ma), and T2 (Upper Cenozoic from 14 Ma to Present) (Figures 2 and 4). They form part of two mega-sequences that result from the major stratigraphic changes during the basin evolution:

i. the Cretaceous mega-sequence and
ii. Cenozoic mega-sequence bound by conspicuous stratigraphic unconformities on the horizons identified by Brown et al. (1995) and Weigelt and Unzelmann-Neben (2004) (Figure 2 and 4).

These sequences can be correlated to their age equivalents defined by previous authors in the southern area of Block 3 and 4 (e.g. Kuhlmann et al., 2010).

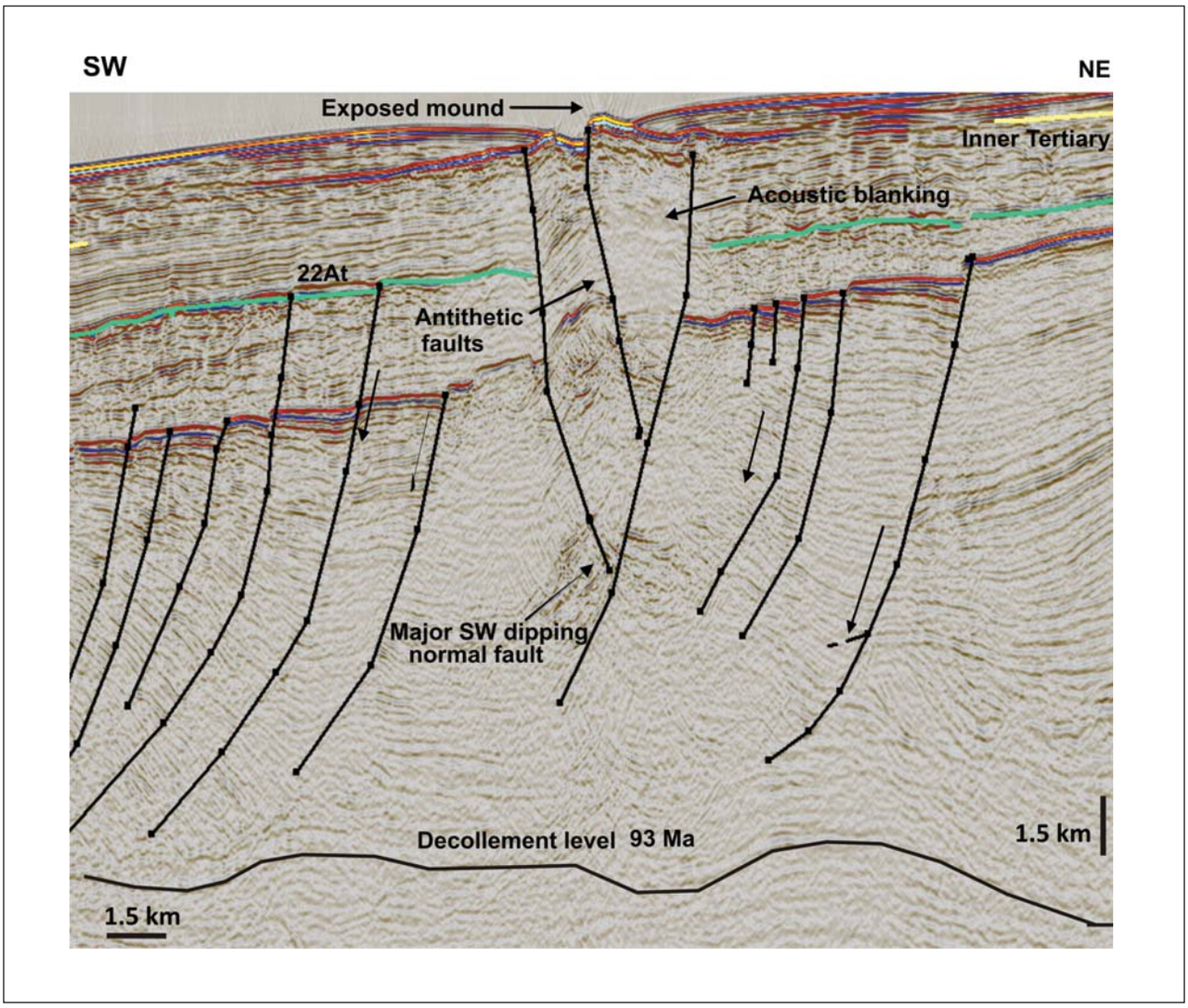

Figure 6. *Close up view of a structurally-controlled chimney that terminates as a seafloor mound with anticline-crestal faulting. The gases migrate up the faults to the exposed mound. The two northeast dipping conjugate faults converge at depth within a major southwest dipping normal fault (black bold lines). The faults are indicated with arrows. Note that the chimney is cut by antithetic faults and the roll-over structures that merge in the décollement zone.*

Our interpretations are consistent with previous work carried out in the Orange Basin (Figure 2). Ten of the horizons identified by Brown et al., (1995) in the Cretaceous period are identified in our study. For example, horizon 6At, at the base of unit C1 is the drift-onset unconformity (Gerard and Smith 1982: Figure 2) and the base of unit C2 is the onset of the drift sequence that is the 13At unconformity (Kuhlmann at al., 2010; Figure 2). This corresponds to the major lithofacies change from restricted marine to open marine conditions. In turn, 22At marks the erosional termination at the base of a Cenozoic wedge that has well-developed prograding clinoforms (Hirsch at al., 2009).

Major structural styles

We observe a distribution of structures across the continental margin that clearly defines two structural domains:

1. an extensional domain along the inner margin; and
2. a compressional domain on the outer margin and deeper part of the basin (Figure 4).

The extensional domain is located on the present-day shelf-break/upper slope between 500 to 1500 m depth (Figure 4). This domain is characterised by basinward dipping listric normal faults that are rooted within a decollement shale layer at the base of the Cretaceous C3 unit, in the Cenomanian– Turonian layer (the 15At reflector; 93 Ma) (Séranne and Anka, 2005; Kuhlmann et al., 2010). The compressional domain is located on the lower slope in the deeper part of the basin, downdip from the above described extensional domain. It is characterized by landward dipping asymmetrical thrusts that apparently accommodate the deformation in up-dip extension domain (Figure 4).

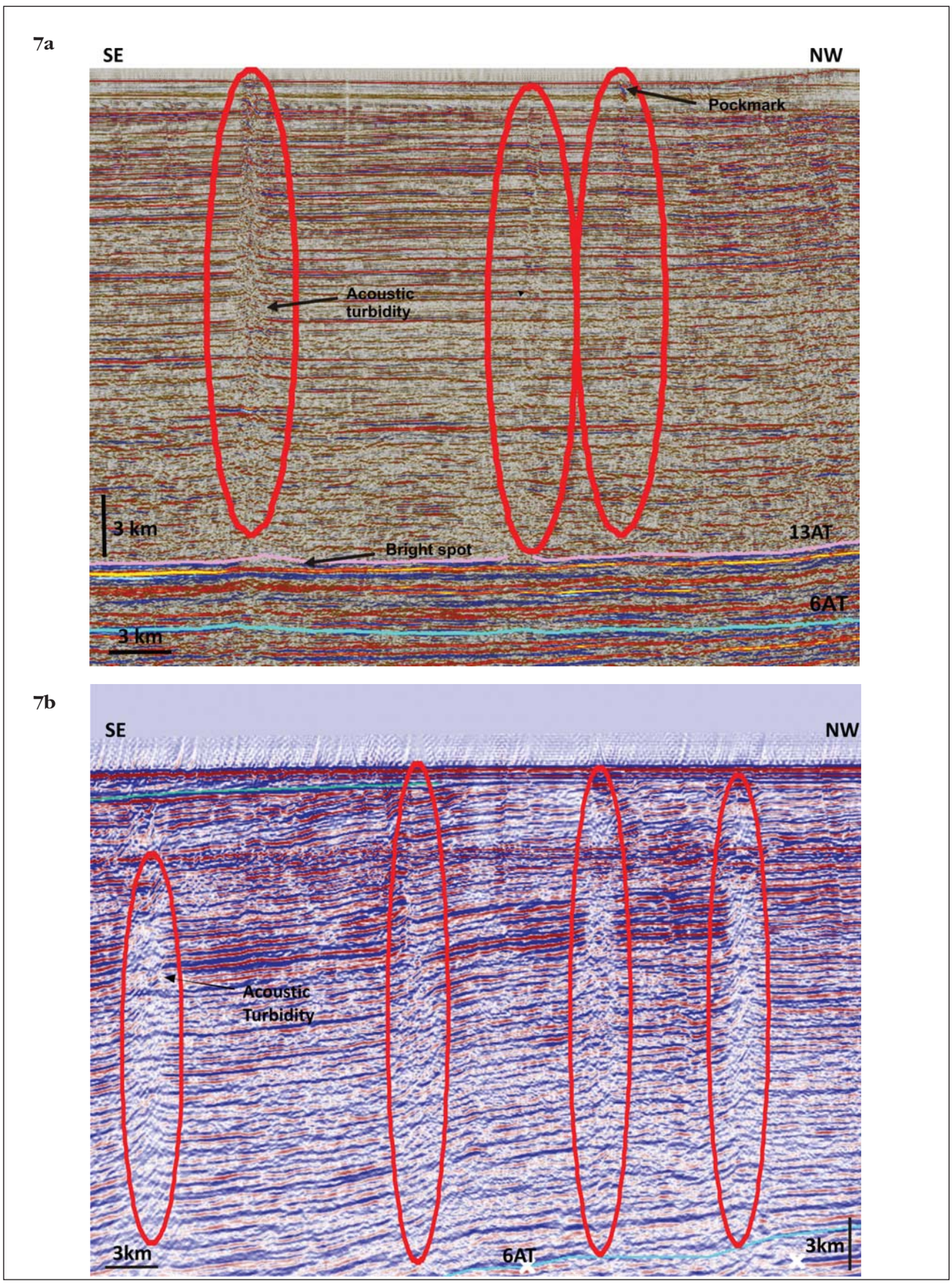

Figure 7. *(**a**) and (**b**) Active stratigraphically-controlled chimneys along the middle margin of the Orange Basin. Note how free gases migrate through the sedimentary column from the Aptian layer (13At) and the lack of faulting. The bright spots indicate the presence of hydrocarbons trapped close to the surface. The pockmarks are about 300 m wide.*

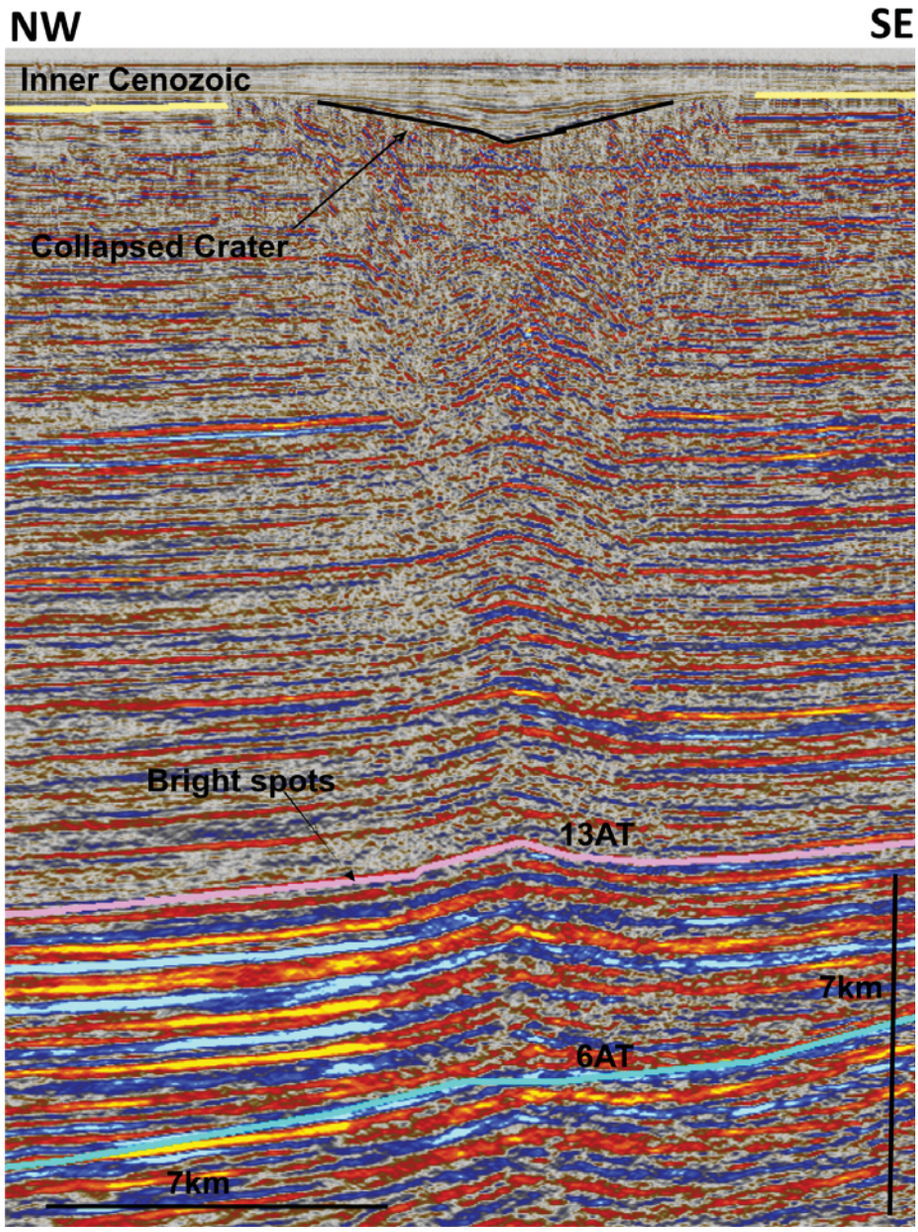

Figure 8. *Giant chimney terminating in a collapse crater of more than 7 km in diameter. Note the lateral bright spots in the lower sections of the chimney and the absence of internal seismic "pull-downs".*

Most of the major faults identified on the outer margin cut through the upper Cretaceous (C3-5) and Cenozoic (T1-2) units, and result from gravitational tectonics along the slope area (e.g. Brown 1993; Butler and Paton 2010). The faults commonly converge at depth within a major southwest dipping normal fault (Viola et al., 2005). Determining factors for the occurrence and style of the gravitational tectonics along the margin may be linked to an increase sedimentation rates and margin tilting (Tinker et al., 2008; Butler and Paton 2010; de Vera et al., 2010). It also appears that episodes of gravitational slumping are related to sea level changes that would have enhanced the progradation of the sediments built up at the slope (Séranne and Anka, 2005; Kuhlmann et al, 2010), or changing ocean currents such as at the onset of the Benguela current (Wiegelt and Unzelmann-Neben, 2004).

Distribution and classification of gas leakage indicators

Many possible indicators of past or active natural hydrocarbon leakage were identified within the study area (Figure 5a and b). These natural gas leakage

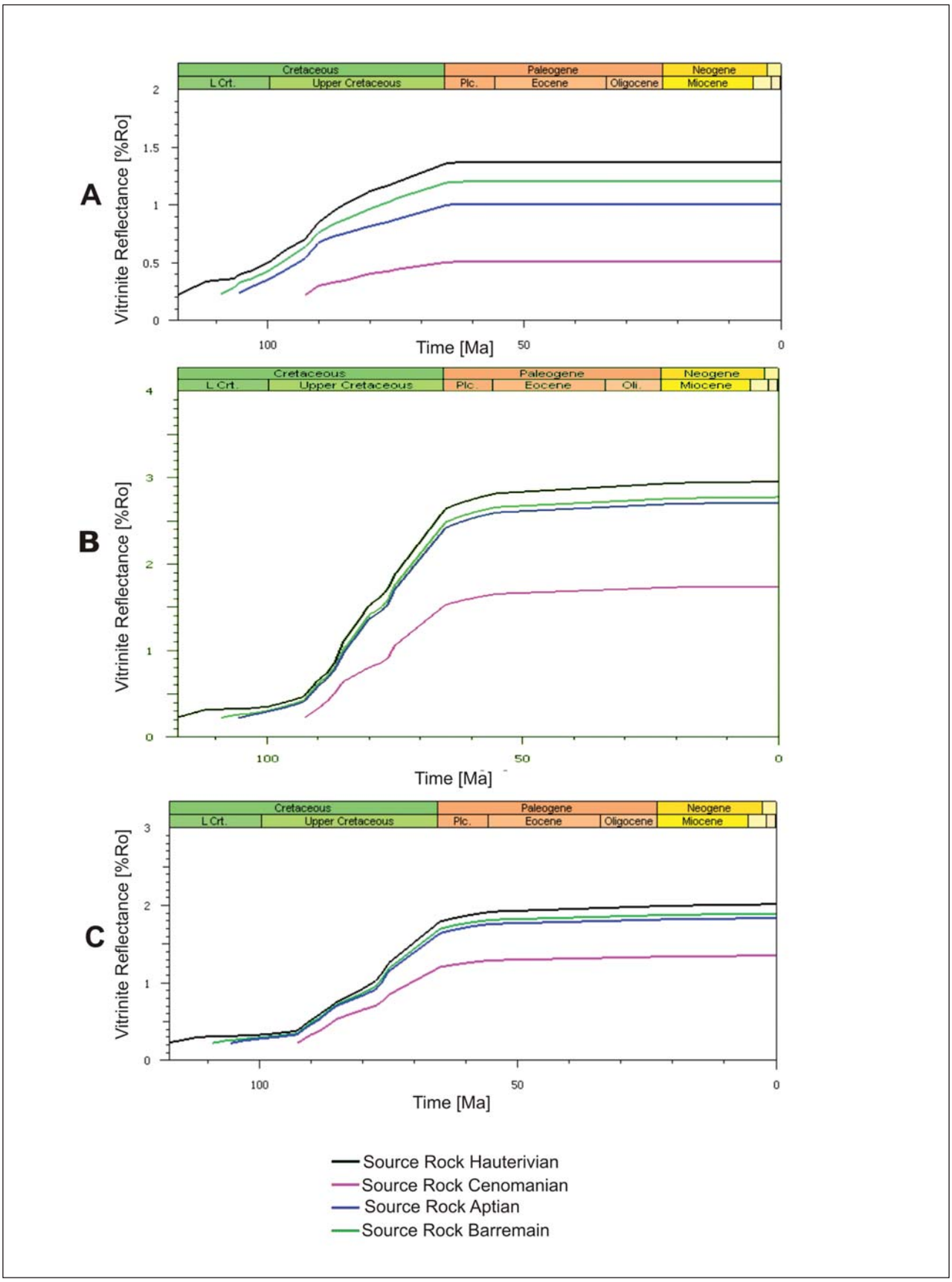

Figure 9. *Model of the vitrinite variation over time in all four source rocks at locations (**A**) (proximal), (**B**) (middle) and (**C**) (distal). All four source rocks start to mature in the early Cretaceous, reaching a maximum maturity at the late Cretaceous, after which there is no further maturation. The Cenomanian/Turonian source rocks is the least mature and the Hauterivian source rocks is the most mature.*

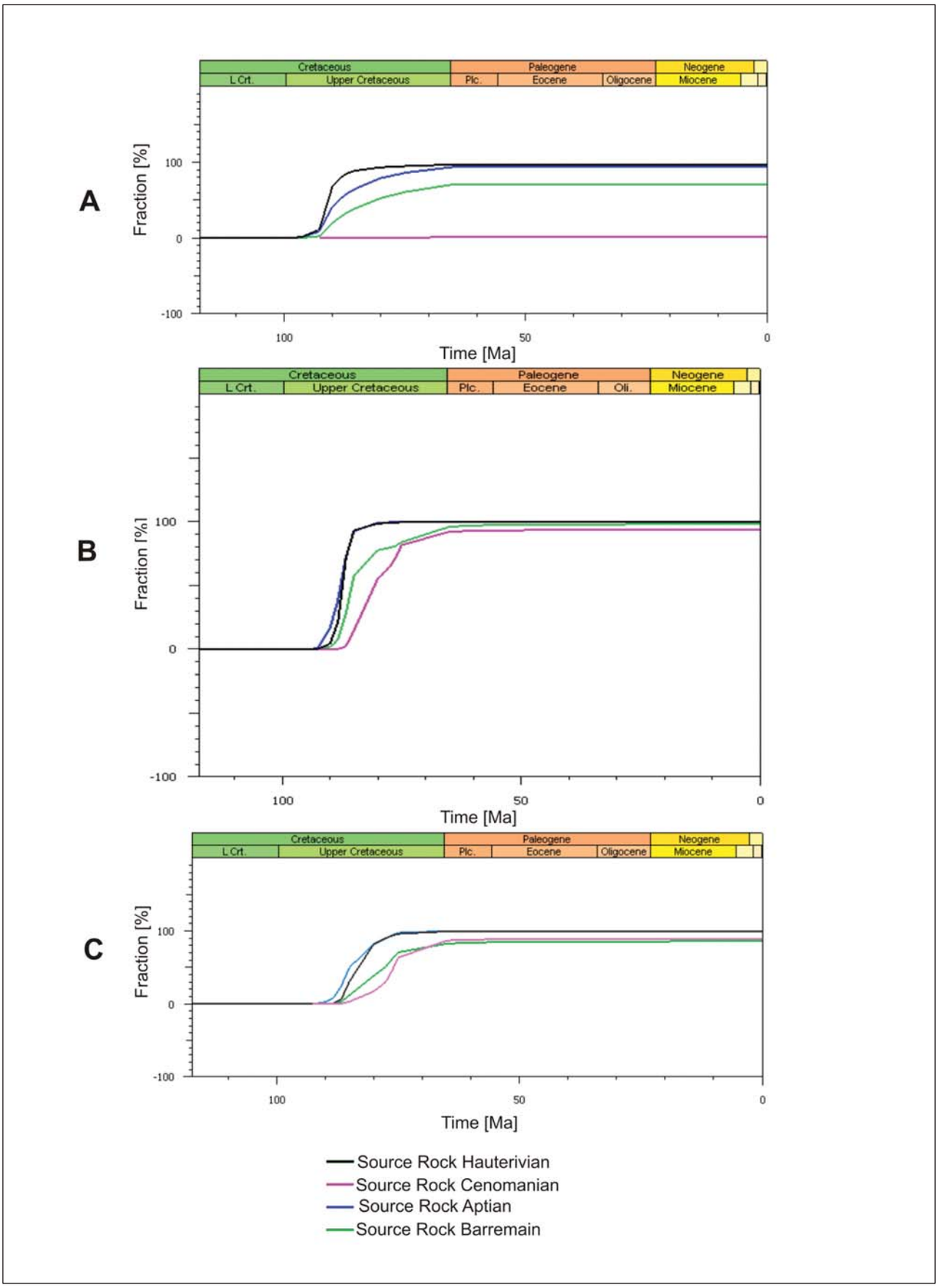

Figure 10. *Model of maturation of all four source rocks at locations (**A**, **B** and **C**) (Figure 8). Note the major step in the Hauterivian source rock (black line), which has the highest transformation ratio.*

Table 1. Source rock kinetic descriptions used in the models

Source rocks	Kinetics for Model 1 (kerogen-oil and gas)	Kinetics for Model 2 (compositional for phase separation)
SR Cenomanian	Pepper&Corvi(1995)_TII(B)	Botneheia_Svalbard_TII_Crack
SR Aptian	Pepper&Corvi(1995)_TII-S(A)	Botneheia_Svalbard_TII_Crack
SR Barremian	Pepper&Corvi(1995)_TIIIH(DE)	Handil_mahakamDelta_TIII_Crack
SR Hauterivian	Pepper&Corvi(1995)_TI(C)	Toarican_ParisBasin_TI_Crack

features occur on the seafloor as pockmarks, mounds, within the stratigraphic column as seismic chimneys or as buried pockmarks. Additionally, several anomalous high amplitude seismic characteristics of gas presence were identified (e.g. bright and flat spots, seismic blanking).

Depending on their association to structural or stratigraphic elements, the gas chimneys are classified into two main categories:

1. structurally-controlled (s-c: Figure 5a and b); and
2. stratigraphically-controlled (s-ac).

The structurally-controlled (s-c) chimneys are all located within the extensional domain (Figure 5b) and appear to originate upwards from the listric normal faults (Figure 6). The existence of these s-c gas leakage features in the deeper parts of the basin, has not to the best of our knowledge- been reported before. The structurally controlled chimneys are located on top of flower structures, mounds and extensional-fault clusters. Approximately, thirty eight of the s-c chimneys are sealed within the Miocene sequence, below the Inner Cenozoic Horizon (Figure 4 and appendix). When the chimneys were buried, this presumably shut off the gas leaking to the hydrosphere. The ratio of s-c versus s-ac chimneys is estimated as 2:5, which suggest a strong stratigraphic control on natural gas leakage in the basin. Chimneys that reach the sea floor terminate either in pockmarks or in seafloor mounds. The latter are up to 1500 m in diameter and between 10 to 50 m in height (Figure 6). Ben-Avraham et al., (2002) previously reported evidence of Bottom Simulating Reflectors (BSR). A BSR is a sub-seafloor phenomenon that marks the boundary between sediments containing gas hydrates from free gas with higher and lower seismic velocities, respectively (Ben-Avraham et al., 2002). BSRs generally have inverse polarity and are parallel to the sea floor reflectors (Rodrigo et al., 2009). During this study, no BSR was detected during this study, or farther to the south (Kuhlmann et al., 2010). However a BSRs was proposed by Ben-Avraham et al. (2002). In our case are not parallel to the seafloor and have the same polarities.

Earlier studies in southern Blocks 3 and 4 revealed the presence of stratigraphically-controlled gas chimneys on the shelf and upper slope, in water depths up to 500 m (Kuhlmann et al., 2010). Similarly, in this study, the sa-c chimneys are identified mostly on the middle and upper shelf in water depths up to 500 m (sa-c: Figures 5a and b and Figures 7a and b). The chimneys appear to be mostly related to the presence of stratigraphic onlaps and pinch-outs within the Aptian sequence, and display no relationship to surrounding faults or other structural features (Figures 7a and b). In this context, either the seal rock is broken at these stratigraphic boundaries or the height of the gas column overcomes the capillary pressure of cap rocks (e.g. Kaluza and Doyle., 1996), allowing the gaseous hydrocarbons to migrate "freely" upward through the sedimentary column. Where the gases are expelled at the seafloor they form pockmarks whose sizes range between 100 to 400 m in diameter. Otherwise the gases are trapped within the sediments close to the sea floor and are detected as seismic bright spots (Figure 7).

At least three giant chimneys were found located beneath the middle shelf (Figure 5a and b and 8). The largest of these features presents an upper diameter of 7 km (Figure 8). Indications of internal gravitational collapse are identified within the chimney of the large craters, which suggests that this structure may result from the collapse of smaller coalescent chimneys.

The giant chimneys have pseudo-conical shapes, with near surface diameters of up to 7.5 km and lower stems of about 2 km. They are sealed within the

Table 2. Hydrocarbons accumulated, expelled and lost at model boundaries (outflow) in megatonnes (10^9 kg)

Model 1	Gas	Oil	Total
Sum expelled	681.68	2727.0	3408.6
Sum accumulated in reservoir	104.56	10.63	115.18
Sum outflow top	778.53	1183.7	1962.2
Sum outflow side	240.43	726.92	967.35
Model 2	**Sum accum. in reservoir**	**Sum outflow top**	**Sum outflow side**
Methane	80.74	245.38	368.82
Ethane	4.19	46.15	43.65
Propane	4.4	47.93	44.84
i-Butane	0.64	7.21	6.6
n-Butane	2.99	32.19	29.55
i-Pentane	2.26	23.6	22.59
n-Pentane	2.11	21.01	20.85
C6	6.55	73.19	62.25
PK_P10	8.93	443.87	321.52
PK_P20	4.67	339.59	240.28
PK_P30	1.58	158.03	119.53
PK_P40	0.4	57.54	54.25
PK_P50	0.08	16.94	22.75
PK_P60+	0.03	6.59	13.46
Sum	119.56	1519.21	1370.93

Miocene section (14 Ma), below the ICH, and do not reach the seafloor. Termination of the gas chimneys seems to result from rapid burial due to slumping. It has been suggested these slump events were related to the onset of the Benguela Current during the Middle Miocene (Weigelt and Unzelmann-Neben., 2004). This current is also responsible for major depositional changes such as slumping, submarine erosions, and contourites deposits in basins farther north along this African continental margin (Séranne and Abeigne, 1999; Weigelt and Unzelmann-Neben., 2004; Séranne and Anka., 2005).

There is no evidence of acoustic turbidity or seismic pull-downs within the chimney tubes, which rules out present-day active upward gas migration from the giant vents. There is therefore no evidence of present gas leakage from the giant vents to the sea floor, despite some bright spots that were identified flanking these structures. It is not clear whether these large paleo structures were stratigraphically-controlled (Sa-c) or if they were linked to deep faulting, because the seismic record does not penetrate deep enough. Although observing Figure 8, the chimney seems to be rooted at ~1750 msec suggesting gas accumulation and release at that level, the detailed analysis on this 'giant chimney' is currently ongoing and is beyond the scope of the paper.

Hydrocarbon Generation and Migration

The evolution of vitrinite reflection (i.e. maturity) of all four source rocks (Figure 9) was extracted from the model for locations A, B, and C (proximal, middle and

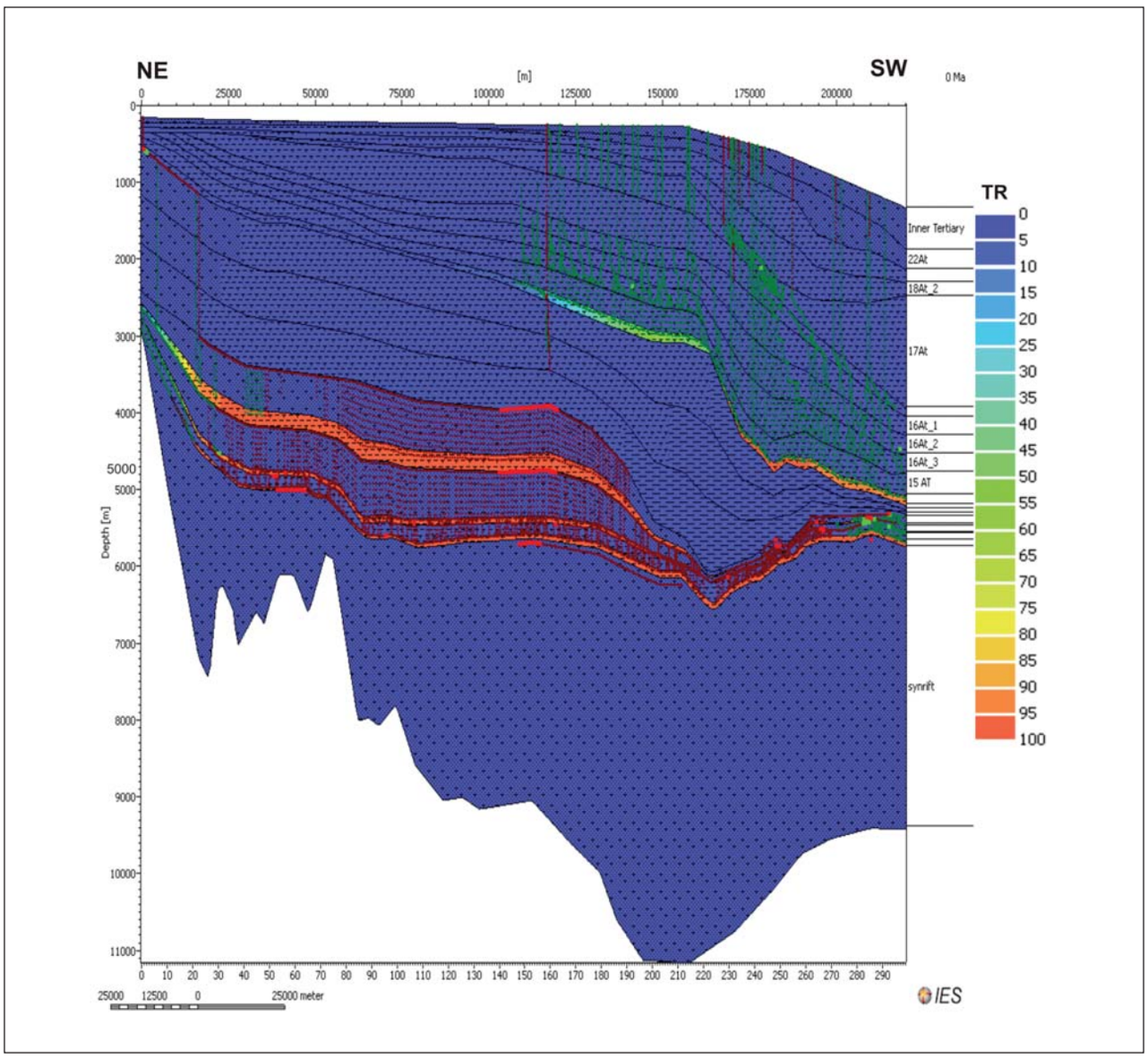

Figure 11. *Migration paths and degree of kerogen conversion (Transformation Ratio) for Model 2. The dotted lines show the migration paths (gases=red and liquids=green). The colour ranges in the source rock intervals represent the Transformation Ratios (see legend).*

distal parts of basin respectively) shown in Figure 3. In all locations, all source rocks start to mature in the early Cretaceous and reach maximum maturity in the late Cretaceous. The middle part of the basin (Location B) has the highest range of vitrinite reflectance values, reaching up to 3% Ro. The transformation ratios over time for the four source rocks, at all locations, are displayed in Figure 10. As observed in this figure, at location A (the proximal part of the basin), Cenomanian/Turonian source rock transformation ratio is at 0.

Petroleum generation and migration modelling attempts to reproduce observed gas leakage pathways in the basin to provide insights on petroleum migration dynamics and to locate the active source "kitchen" areas. Our fluid-flow modelling assumes invasion percolation as the preferred migration tool for modelling fluid flow (Carruthers and de Lind van Wijngaarden 2000; Figure 3). This approach models flow through focused pathways as a function of the capillary entry pressure field in the sedimentary system and on the timescales of secondary petroleum migration. Hydrocarbon flow is overwhelmingly controlled by the balance between gravity (or buoyancy) and capillary forces. Viscous forces are negligible. Invasion percolation migration occurs mainly when fluids are generated and enter the secondary migration space. At that point, fluids migrate farther through the sedimentary system as a function of hydrocarbon column height and capillary entry pressure until a final balance is reached, whilst other flow models exist (Schneider 2003 and Hantschel et al., 2000)

Our first fluid model (Model 1) reproduces at least two primary processes responsible for gas leakage across the basin (Figure 3). The first is petroleum migration that occurs in the lower shelf where significant faulting occurs. The second starts in the middle and upper shelf where the leakage is associated with vertical migration of free gas, despite the apparent absence of significant faulting.

Hydrocarbons generated from the older marine source rocks of the Lower Aptian and Barremian age migrate up-dip beneath the seals towards the proximal end of the basin. The locations of the predicted hydrocarbon accumulations coincide with bright spots identified in the seismic profiles (Figure 3). When the gases have migrated to the proximal part of the basin, they subsequently leak to the sea floor in response to a change in the overlying lithologic properties (e.g. from siltstone to sandstone, Figure 3).

Hydrocarbons migrating to the shelf break and to the distal part of the basin are fed by younger source rocks of Cenomanian/Turonian age. No hydrocarbons from the younger source rocks are found to leak from the proximal part of the basin. To predict the position of other leakage sites, a 3D modelling approach is required, which is beyond the scope of this work. The 2D basin modelling can, however, successfully assess semi-quantitatively the extent of hydrocarbon generation, expulsion, migration, accumulation and cracking of the generated petroleum in the system studied.

A second model (Model 2) was created using compositional kinetics, that is based on the PhaseKinetic technique described by di Primio and Horsfield (2006); Table 1). This approach allows a more realistic reproduction of hydrocarbon compositional evolution as a function of primary and secondary cracking as well as the correct simulation of hydrocarbon phase behaviour during migration. The difference between the two models is due to the different kinetic schemes applied and their control on the timing and extent of hydrocarbon generation from the source rocks. Overall, the migration paths result from modeling and not the input data.

Comparisons between the two models show:

1. fluids in Model 1 migrate predominantly subvertically towards the surface rather than sub-horizontally (1962.23 and 967.35 Mtons, respectively, Table 2),
2. fluids in Model 2 also flow subvertically upwards yet they do so, only marginally more than those that migrate subhorizontially (1519.21 to 1370.93 Mtons, respectively Table 2).

The differences are largely due to the physical properties of the oil and gas phases modelled (i.e. density). Both models predict that the fluids are 24 to 25 times more likely to flow out of the Orange Basin than to be preserved within it.

In the final analyses, Model 2 best fits the petroleum systems of the Orange Basin, bearing in mind that both models can be improved by increasing data input from the seismic data (e.g. facies constraints). Although, results of migration Model 1 (Figure 3) and Model 2 (Figure 11) both accurately produce the spatial associations of the identified gas chimneys in the TWT seismic sections, the migration paths in Model 2 (Figure 11) are simpler and, unlike Model 1, shows migration of gases in the deep sections of the basin. These deep-sourced gases migrate from the mature source (kitchen) interval of Cenomanian/Turonian age with a TR ranging from 88% in the distal sectors of the basin (Figure 11). Since Model 2 makes more predictions consistent with what is observed in the seismic data, this is our preferred final model.

Conclusions and perspectives

This work has provided clues about the controlling factors for gas mobility leakage out of the Orange Basin. 2D petroleum modelling has provided, for the first time, clarity on the timing of gas generation, migration and sequestration dynamics; and it has revealed the maturation history for the west-east transect across the basin. The major findings from this work can be summarized as follows:

- The two main tectonic regimes are:

1. an extensional domain flanking the inner margin, characterised by basinward dipping listric normal faults rooted in the décollement layer (Cenomanian–Turonian layer)

2. a compressional domain on the outer margin and deeper parts of the basin, characterized by landward dipping asymmetrical thrusts, which apparently accommodate the deformation in up-dip extension domain.

- Several gas leakage indicators were identified on the middle shelf and lower shelf of Block 2. They are controlled either by stratigraphic or structural elements. The structurally-controlled chimneys originate along normal listric faults of the extensional domain. The stratigraphically-controlled chimneys are linked to the presence of onlaps and pinch-outs within the Aptian sequence.
- Large paleo escape structures such as giant chimneys, with more than 7 km diameter, are observed in the middle margin of the Orange Basin. These structures were covered by sediments at ca. 14 Ma (Miocene). This is possibly due to rapid burial during slumping during the onset of the cold Benguela Current (Weigelt and Ünzelmann-Neben., 2004; Séranne and Anka., 2005). Shut-down of these gas escape structures would have terminated fluid escape. This event, if integrated over the entire South African continental margin, may have contributed to the Neogene global cooling, but better quantification is needed to verify this (e.g. Ruddiman 2010).
- The source rocks of Early Cretaceous age have reached generally high levels of conversion, and at the present time are generating gas that migrates laterally to the proximal part of the basin, after which vertical migration dominates.
- The Late Cretaceous source rocks show only high levels of conversions to hydrocarbon fluids in the deep part of the basin. Migration of generated gas is limited to the shelf break and deeper part of the basin. The migration pathways are apparently linked to the stratigraphic-controlled (sa-c) and structural-controlled (s-c) chimneys mapped in the upper and middle shelves of the basin, respectively. The gas migrates up-dip along the basinward dipping listric faults of the extensional domain that are rooted in a décollement of Upper Cretaceous source rock. Thus, there is an intimate connection between the source rocks and gas leakage at the surface via the identified chimneys.

Overall, the total global volume of methane leaking to the seafloor from continental margins is unknown. Clearly challenges remain ahead, particularly because only very few passive margins have been investigated for gas escape structures. However, this work shows that the deep-sourced methane contributions from the Orange Basin to the atmosphere and their possible effects on paleo-climate evolution was non-linear and must have varied substantially through time. This work provides a model of the Orange Basin that enhances understanding on how, where and why the gases in this basin are generated, and how they migrate and leak relative to the structural and stratigraphic elements of the basin. Continuation of this type of work will provide further understanding on the relationship of methane migration and seepage with structural and stratigraphic elements, as well as on the timing and amounts of gas leakage to the exosphere from sedimentary basins worldwide. In turn, they may lead to a better understanding of the role of basin fluids to past climate changes.

Acknowledgements

This study is an Inkaba yeAfrica project, supported by African Earth Observatory Network (AEON), University of Cape Town, and GFZ German Research Centre for Geosciences, Potsdam. We are grateful for PASA for providing the data and for permission to publish the results, and National Research Foundation (NRF) for funding. Thanks also for constructive review by journal referees Zvi Ben-Avraham and Douglas Paton. This is an Inkaba ye Africa publication No. 49 and AEON contribution 87.

References

Barton, K.R., Muntingh, A. and Noble, R.D.P., 1993. Geophysical and geological studies applied to hydrocarbon exploration on the west coast margin of South Africa. Extended abstract of the Third International Congress of the Brazilian Geophysical Society, Rio de Janerio, Brazil. November 7–11 1993.

Ben-Avraham, Z., Smith, G., Reshef, M. and Jungslager, E., 2002. Gas Hydrate and mud volcanoes on the southwest African continental margin off South Africa. Geology, 30, 927–930.

Bray, R., Lawrence, S. and Swart, R., 1998. Source rock, Maturity Data indicates potential off Namibia. Oil and Gas Journal, 96, 84–49.

Brendt, C., 2005. Focused fluid flow in passive continental margins. Philosophical Transactions of the Royal Society, London, A, 363, 2855–2871.

Broad, D.S., Jungslager, E.H.A., McLachlan, I.R. and Roux, J., 2006. Offshore Mesozoic Basins. In: M.R. Johnson, C. R. Anhaeusser and R. J. Thomas (Editors), The Geology of South Africa. Geological Society of South Africa/Council for Geosciences, 553–571.

Brown, Jr., L. F., Benson, J. M., Brink, G. J., Doherty, S., Jollands, A., Jungslager, E. H., Keenen, A., Muntingh, A. and van Wyk, N. J. S., 1995. Sequence stratigraphy in offshore South African divergent basins. An atlas on exploration for Cretaceous lowstand traps by Soekor (Pty) Ltd.: American Association of Petroleum Geologists, Studies in Geology, 41, 184pp.

Bunz, S., Mienert, J., Brynw, P. and Bergw, K., 2005. Fluid flow impact on slope failure from 3D seismic data: a case study in the Storegga Slide. Basin Research, 17, 109–122.

Butler, R.W.H. and Paton, D.A., 2010. Evaluating lateral compaction in deepwater fold and thrust belts: How much are we missing from "nature's sandbox"? GSA Today, 20, 4–10.

Carruthers, D.J. and de Lind van Wijngaarden M., 2000. Modelling viscous-dominated fluid transport using modified invasion percolation techniques. Journal of Geochemical Exploration, 69–70, 669–672.

Cranston, R.E., Ginsburg, G.D., Soloviev, V.A. and Lorenson, T.D., 1994. Gas venting and hydrate deposits in the Okhotsk Sea. Bulletin of the Geological Society of Denmark, 41, 80–85.

Crutzen, P.J., 1991. Methane's sinks and sources. Nature, 350, 380–381.

di Primio, R. and Horsfield, B., 2006. From petroleum-type organofacies to hydrocarbon phase prediction. American Association of Petroleum Geologists, Bulletin, 90, 1031–1058.

de Vera, J., Granado, P. and McClay, K. (2010). Structural evolution of the Orange Basin gravity-driven system, offshore Namibia. Marine and Petroleum Geology, 27, 223–237.

de Wit, M.J., Ghosh, J.G., de Villiers, S., Rakotosolofo, N. and Alexander, J., 2002. Multiple organic carbon isotope reversals across the Permo-Triassic

boundary of terrestrial Gondwana sequences: clues to extinction patterns and delayed ecosystem recovery. Journal of Geology, 110, 227–240.

Dickens, G.R., 2003. Rethinking the global carbon cycle with a large, dynamic and microbially mediated gas hydrate capacitor. Earth and Planetary Science Letters, 213, 169–183.

Dingle, R.V., Siesser, W.G. and Newton, A.R., 1983. Mesozoic and Cenozoic geology of Southern Africa. A.A Balema, Rotterdam, The Netherlands, 355pp.

Dimitrov, L.I., 2002. Mud volcanoes; the most important pathway for degassing deeply buried sediments. Earth-Science Reviews, 59, 49–76.

Etiope, G., 2004. New Directions: GEM-Geologic Emissions of Methane, the missing source in the atmospheric methane budget. Atmospheric Environment, 38, 3099–3100.

Etiope, G., Keith, R.L., Ronald, W.K and Boschi, E., 2008. Reappraisal of the fossil methane budget and related emission from geologic sources. Geophysical Research Letters, 35, 1–5.

Etiope, G. and Klusman, R.W., 2002. Geologic emissions of methane to the atmosphere. Chemosphere, 49, 777–789.

Gerrard, T. and Smith, G.C., 1982. Post-Palaeozoic succession and structure of the south-western African continental margin, In: J.S. Watkins and C.L. Drake (Editors). Studies in Continental Margin Geology. American Association of Petroleum Geologists, Memoir, 34, 49–74.

Gradstein, F., Ogg, J. and Smith, J., 2004. A Geologic Time Scale. Cambridge University Press, United Kingdom, 589pp.

Hantschel, T., Kauerauf, A.I. and Wygrala, B., 2000. Finite element analysis and ray tracing modelling of petroleum Migration. Marine and Petroleum Geology, 17, 815–820.

Herbin, J.P., Muller, C., Graciansky, P.C. de Jacquin, T., Magniez-Jannin, F. and Unternehr, P., 1987. Cretaceous anoxic event in the South Atlantic. Revista Brasileria de Geociencia, 17, 92–99.

Hirsch, K., Scheck-Wenderoth, M., van Wees, J., Kuhlmaan, G. and Paton, D.A., 2009. Tectonic subsidence history and thermal evolution of the Orange Basin. Marine and Petroleum Geology, 27, 565–584.

Judd, A.G., Hovland, M., Dimitrov, L.I., Garcia Gil, S. and Jukes, V., 2002. The geological methane budget at Continental Margins and its influence on climate change. Geofluids, 2, 109–126.

Jungslager, E.H.A., 1999. Petroleum habitats of the Atlantic margin of South Africa, In: N.R. Cameron, R.M. Bate and V.S. Clure (Editors). The oil and gas habitats of the South Atlantic: The Geological Society, London, Special Publication, 153, 153–168.

Kaluza, M.J. and E.H. Doyle., 1996. Detecting Fluid Migration in Shallow Sediments: Continental Slope Environment, Gulf of Mexico. In: D. Schumacher and M.A Abrams (Editors). Hydrocarbon migration and its near surface expression. American Association of Petroleum Geologists, Memoir, 66, 15–26.

Kennett, J.P., Cannariato, K.G., Hendy, I.L. and Behl, R.J., 2002. Methane Hydrates in Quaternary Climate Change: The Clathrate Gun Hypothesis. Washington D.C., American Geophysical Union, 216pp.

Kuhlmann, G., Adams, S., Campher, C., van der Spuy, D., di Primio, R. and Horsfield, B., 2010. Passive margin evolution and its controls on natural gas leakage in the southern Orange Basin, block ¾, offshore South Africa. Marine and Petroleum Geology, 27, 973–992.

MacDonald, D., Gomez-Perez, I., Franzese J., Spalleti, L., Lawver, L., Gahagan, L., Dalziel, I., Thomas, C., Trewin, N., Hole, M. and Paton, D., 2003. Mesozoic break-up of SW Gondwana: implications for regional hydrocarbon potential of the southern South Atlantic. Marine and Petroleum Geology, 20, 287–308.

Mazinni, A., Svensen, H., Hovland, M. and Planke, S., 2006. Comparison and implications from strikingly different authigenic carbonates in a Nyegga complex pockmark, G11, Norwegian Sea. Marine Geology, 231, 89–102.

McElwain, J.C., Wagner, P. and Hesselbo, S., 2009. Fossil plant relative abundances indicate sudden loss of Late Triassic biodiversity in East Greenland. Science, 324, 1554–1556.

McKenzie, D., 1978. Some remarks on the development of sedimentary basins. Earth and Planetary Science Letters, 40, 25–32.

Milkov, A.V., 2004. Global estimates of hydrate-bound gas in marine sediments: How much is really out there? Earth Science Reviews, 66, 183–197.

Moulin, M., Aslanian, D. and Unternehr, P., 2010. A new starting point for the South and Equatorial Atlantic Ocean Earth. Science Reviews, 98, 1–37.

Muntingh, A. and Brown, Jr. L. F., 1993. Sequence stratigraphy of petroleum plays, postrift Cretaceous rocks (lower Aptian to upper Maastrichtain). Orange Basin, western offshore, South Africa. In: P. Weimer and H.W Posamentier (Editoers). Siliciclastic sequence stratigraphy-recent developments and applications. American Association of Petroleum Geologists, Memoir, 58, 71–97.

Nurnberg, D. and Muller, R.D., 1991. The tectonic evolution of the South Atlantic from Late Jurassic to present. Tectonophysics, 191, 27–53.

Pallasser. R.J., 2000. Recognising biodegradation in gas/oil accumulations through the ^{13}C compositions of gas components. Organic Geochemistry, 31, 1363–1373.

Paton, D.A., di Primio, R., Kuhlmann, G., van der Spuy, D. and Horsfield, B., 2007. Insights into the petroleum system evolution of the southern Orange Basin, South Africa. South African Journal of Geology, 110, 261–274.

Paton, D.A., van der Spuy, D., di Primio, R. and Horsfield, B., 2008. Tectonically induced adjustment of passive-margin accommodation space; influence on the hydrocarbon potential of the Orange Basin, South Africa. American Association of Petroleum Geologists, Bulletin, 92, 589–609.

Pepper, A.S. and Corvi, P.J., 1995a. Simple kinetic models of petroleum formation. Part I: oil and gas generation from kerogen. Marine and Petroleum Geology, 12, 291–319.

Pepper, A.S. and Corvi, P.J., 1995b. Simple kinetic models of petroleum formation. Part III: Modelling an open system. Marine and Petroleum Geology, 12, 417–452.

Pepper, A.S. and Dodd, T.A., 1995. Simple kinetic models of petroleum formation. Part II: oil to gas cracking. Marine and Petroleum Geology, 12, 321–340.

Petroleum Agency SA., 2003. South African exploration opportunities. South African Agency for Promotion of Petroleum Exploration and Exploitation, Parrow, Cape Town, 28pp.

Poelchau, H.S., Baker, D.R., Hantschel, T., Horsfield, B. and Wygrala, B., 1997, Basin simulation and the design of the conceptual model. In: D.H. Welte, B. Horsfield and D.R. Baker (Editors). Petroleum and Basin Evolution, Springer, Berlin, Germany, 3–69.

Rodrigo, C., Vera, E. and González-Fernández, A., 2009. Seismic analysis and distribution of a bottom-simulating reflector (BSR) in the Chilean margin offshore of Valdivia (40° S). Journal of South American Earth Sciences, 27, 1–10.

Royer, D.L., 2006. CO2-forced climate thresholds during the Phanerozoic. Geochimica, 70, 5665–5675.

Royer, D.L., Berner, R.B., and Park, J., 2007. Climate sensitivity constrained by CO_2 concentrations over the past 420 million years. Nature, 446, 530–532.

Ruddiman, W.F., 2010. A Paleoclimatic Enigma? Science, 328, 838–839.

Séranne, M., Abeigne, C. -R. Nzé. and Lopez, M., 1999. Oligocene to Holocene sediment drifts and bottom-currents on the slope of Gabon continental margin (West Africa). Consequences for sedimentation and southeast Atlantic upwelling. Sedimentary Geology, 128, 179–199.

Séranne, M. and Anka, Z., 2005. South Atlantic continental margins of Africa: A comparison of the tectonic vs climate interplay on the evolution of equatorial West Africa and SW Africa margins. Journal of African Earth Sciences, 24, 283–300.

Schneider, F., 2003. Modelling multiphase flow of petroleum at the sedimentary basin scale. Journal of Geochemical Exploration, 78–79, 693–696.

Svensen, H., Jamtveit, B. and Planke, S., 2003. Seep carbonate formation controlled by hydrothermal vent complexes: a case study from the Vøring volcanic basin, the Norwegian Sea. Geo-Marine Letters, 23, 351–358.

Svensen, H., Planke, S., Malthe-Sørenssen, A., Jamtveit, B., Myklebust, R., Rasmussen Eidem, T. and Rey, S.S., 2004. Release of methane from a volcanic basin as a mechanism for initial Eocene global warming. Nature, 429, 542–545.

Sweeney, J.J. and Burnham, A.K., 1990. Evaluation of a Simple Model of Vitrinite Reflectance Based on Chemical Kinetics. American Association of Petroleum Geologists, Bulletin, 74, 1559–1570.

Tinker, T., de Wit, M. and Brown, R., 2008. Linking source and sink: Evaluating the balance between onshore erosion and offshore sediment accumulation since Gondwana break-up, South Africa. Tectonophysics, 455, 94–103.

Trumbull, R. B., Reid, D. L., de Beer, C., van Acken, D. and Romer, R.L., 2007. Magmatism and continental breakup at the west margin of southern

Africa: A geochemical comparison of dolerite dikes from northwestern Namibia and the Western Cape. South African Journal of Geology, 110, 477–502.

Uenzelmann-Neben, G., Schlüter, P. and Weigelt, E., 2007. Cenozoic oceanic circulation within the South African gateway: indications from seismic stratigraphy. South African Journal of Geology. 110, 275–294.

Van de Schootbrugge, B., Payne, J.L., Tomasovych , A., Pross, J., Fiebig, J., Benbrahim, M., Follmi, K.B. and Quan, T.M., 2008. Carbon cycle perturbation and stabilization in the wake of the Triassic-Jurassic boundary mass-extinction event. Geochemistry, Geophysics, Geosystems, 9, 1–16.

Van der Spuy, D., Ziegler, T. and Bowyer, M., 2003. Deepwater 2D data reveal Orange Basin objectives off western South Africa. Oil and Gas Journal, 101, 44–49.

Viola, G., Andreoli, M., Ben-Avraham, Z., Stengel, I. and Reshef, M., 2005. Offshore mud volcanoes and onland faulting in southwestern Africa: neotectonic implications and constraints on the regional stress field. Earth and Planetary Science Letters, 231, 147–160.

Waples, D., 2000. The kinetics of in-reservoir oil destruction and gas formation: constraints from experimental and empirical data, and from thermodynamics. Organic Geochemistry, 31, 553–575.

Weigelt, E. and Unzelmann-Neben, G., 2004. Sediment deposits in the Cape Basin: Indications for shifting ocean currents? American Association of Petroleum Geologists, Bulletin, 88, 765–780.

Westerhold, T., Bickert, T. and Röhl, U., 2005. Middle to late Miocene oxygen isotope stratigraphy of ODP site 1085 (SE Atlantic): new constrains on Miocene climate variability and sea-level fluctuations, Palaeogeography, Palaeoclimatology, Palaeoecology, 217, 205–222.

Whiticar, M.J., 1989. A geochemical perspective of natural gas and atmospheric methane. Advances in Organic Geochemistry, 16, 531–547.

Wuebbles, D.J. and Hayhoe, K., 2002. Atmospheric methane and global change. Earth-Science Reviews, 57, (3-4), 177–210.

Wygrala, B.P., 1989. Integrated study of an oil field in the southern Po basin, northern Italy. Forschungs zentrum Jülich reports, 2313, 217pp.

Zachos, J.C., Dickens, G.R and Zeebe, R.E., 2008. An early Cenozoic perspective on greenhouse warming and carbon-cycle dynamics. Nature, 451, 279–283.

Editorial handling: Robert Trumbull